

ON THE IMPROVEMENT OF THE TOPOLOGICAL ACTIVE VOLUMES MODEL

A Tetrahedral Approach

N. Barreira, M. G. Penedo, M. Ortega and J. Rouco
VARPA Group, Department of Computer Science, Universidade da Coruña, Spain
{nbarreira, mgpenedo, mortega, jrouco}@udc.es

Keywords: 3D Image Segmentation, Deformable models, Active models, Topological Active Volumes.

Abstract: The Topological Active Volumes model is a 3D active model focused on segmentation and reconstruction tasks. The segmentation process is based on the adjustment of a 3D mesh composed of polyhedra. This adjustment is guided by the minimisation of several energy functions related to the mesh. Even though the original cubic mesh achieves good segmentation results, it has difficulties in some cases due to its shape. This paper proposes a new topology for the TAV mesh based on tetrahedra that overcomes the cubic mesh difficulties. Also, the paper explains an improvement in the tetrahedral topology to increase the accuracy of the results as well as the efficiency of the overall process.

1 INTRODUCTION

Deformable models are well-known tools for image segmentation and reconstruction. They were introduced in 2D by Kass et al. (Kass et al., 1988) and generalised to 3D by Terzopoulos et al. (Terzopoulos et al., 1988). The active nets model was first proposed by Tsumiyama and Yamamoto (Tsumiyama and Yamamoto, 1989) as a variant of the deformable models that integrates features of region-based and boundary-based segmentation techniques. To this end, this model has two different kind of nodes: internal nodes, for modelling the inner topology, and external nodes, for surface adjustment. The former is related to the region information whereas the latter uses boundary information. The Topological Active Volumes (TAV) model (Barreira and Penedo, 2005) is a 3D extension of the active nets model. It has an advantage over other models since it not only fits the surfaces but also models the whole volume. A TAV consists of a set of nodes organised in a polyhedral mesh. Just like any other deformable model, the mesh deformation is guided by energy functions in such a way that the mesh energy has a minimum when the model is over the objects of the scene. Also, the TAV model is able to perform topological changes in its structure in order to adjust to concavities, detect holes, and find separate objects in the scene.

The TAV model, originally developed as a cubic mesh, achieves good segmentation results in both synthetic and real images (Barreira and Penedo, 2004). The cubic mesh is simple and able to adapt to a wide range of surfaces. However, in objects with pronounced curvatures, the cubic mesh has difficulty in the adjustment due to the four-sided faces of the cubes. In these cases, a tetrahedral mesh could fill the space better and, thus, improve the results. Since tetrahedral meshes are widely used in modelisation and reconstruction (Archip et al., 2006; Sitek et al., 2006) as well as in segmentation tasks with deformable models (Sermesant et al., 2003; Pons and Boissonnat, 2007), this paper proposes a new mesh topology for the TAV model based on tetrahedra. The development of a mesh topology is not straightforward and implies new ways of initialising and performing topological changes in the structure. Also, since the new node relationships affect the calculus of the energies, they have influence on the computation times. For this reason, some improvements were developed in order to increase the efficiency of the model.

This paper is organised as follows. Section 2 explains the characteristics of the model and the segmentation process. Section 3 introduces the tetrahedral topology as well as the strategy developed to improve the results. Section 4 shows some results of the

new topology. Finally, section 5 explains the conclusions and the future work.

2 MODEL

A Topological Active Volume (TAV) is a three-dimensional structure composed of interrelated nodes located at the vertices of a polyhedron (Barreira and Penedo, 2005). This polyhedron is repeated throughout the mesh and defines the neighbouring relationships among nodes. There are two types of nodes: internal, inside the mesh, and external, on the surfaces. Each type of node represents different object features. The external nodes fit the surface of the object whereas the internal nodes model its inner topology. Figure 1 depicts a TAV where the repeated polyhedron is a cube.

Parametrically, a TAV is defined as $v(r, s, t) = (x(r, s, t), y(r, s, t), z(r, s, t))$, where $(r, s, t) \in ([0, 1] \times [0, 1] \times [0, 1])$. The state of the model is governed by an energy function defined as follows:

$$E(v) = \int_0^1 \int_0^1 \int_0^1 E_{int}(v(r, s, t)) + E_{ext}(v(r, s, t)) dr ds dt \quad (1)$$

where E_{int} and E_{ext} are the internal and the external energy of the TAV, respectively. The former controls the shape and the structure of the net. Its calculus depends on first and second order derivatives which control contraction and bending, respectively. The internal energy term is defined by:

$$E_{int}(v(r, s, t)) = \alpha(|v_r(r, s, t)|^2 + |v_s(r, s, t)|^2 + |v_t(r, s, t)|^2) + \beta(|v_{rr}(r, s, t)|^2 + |v_{ss}(r, s, t)|^2 + |v_{tt}(r, s, t)|^2) + 2\gamma(|v_{rs}(r, s, t)|^2 + |v_{rt}(r, s, t)|^2 + |v_{st}(r, s, t)|^2) \quad (2)$$

where subscripts represent partial derivatives and α , β and γ are coefficients that control the smoothness of the net. In order to compute the energy, the parameter domain $[0, 1] \times [0, 1] \times [0, 1]$ is discretized as a regular grid defined by the internode spacing (k, l, m) and the first and second derivatives are estimated using the finite differences technique in 3D.

E_{ext} represents the characteristics of the scene that guide the adjustment process and is defined as follows:

$$E_{ext}(v(r, s, t)) = \omega f[I(v(r, s, t))] + \frac{\rho}{|\mathfrak{N}(r, s, t)|} \sum_{p \in \mathfrak{N}(r, s, t)} \frac{1}{\|v(r, s, t) - v(p)\|} f[I(v(p))] \quad (3)$$

where ω and ρ are weights, $I(v(r, s, t))$ is the intensity value of the original image in the position $v(r, s, t)$, f is a function related to the image intensity, and $\mathfrak{N}(r, s, t)$ is the neighbourhood of the node (r, s, t) . This way, given that the repeated polyhedron in the mesh defines the node neighbourhoods, the shape of

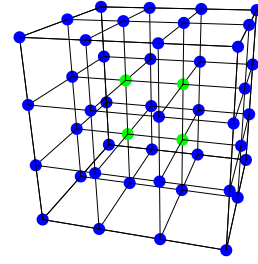


Figure 1: A $4 \times 4 \times 3$ TAV mesh where the base polyhedron is a cube. The dark nodes represent the external nodes whereas the light ones are the internal nodes.

the polyhedron influences not only the flexibility of the mesh, but also the way the nodes are adjusted to the objects.

Since the internal and external nodes model different parts of the objects, f should be adapted for both types of nodes. On one hand, if the objects to detect are dark and the background is light, the energy of an internal node will be minimum when it is on a point with a low grey level. On the other hand, the energy of an external node will be minimum when it is on a discontinuity and on a light point outside the object. In this situation, function f is defined as:

$$f[I(v)] = \begin{cases} h[\overline{I(v)_n}] & \text{for internal nodes} \\ h[I_{max} - \overline{I(v)_n}] + \xi(G_{max} - G(v)) + GD(v) & \text{for external nodes} \end{cases} \quad (4)$$

where ξ is a weighting term, I_{max} and G_{max} are the maximum intensity values of image I and the gradient image G , respectively, $I(v)$ and $G(v)$ are the intensity values of the original image and the gradient image in the node position $v(r, s, t)$, $\overline{I(v)_n}$ is the mean intensity in a $n \times n \times n$ cube, h is an appropriate scaling function, and $GD(v)$ is the gradient distance, this is, the distance from the node position $v(r, s, t)$ to its nearest edge.

Otherwise, if the objects are bright and the background is dark, the energy of an internal node will be minimum when it is on a point with a high grey level and the energy of an external node will be minimum when it is on a discontinuity and on a dark point outside the object. In such a case, function f is defined as:

$$f[I(v)] = \begin{cases} h[I_{max} - \overline{I(v)_n}] & \text{for internal nodes} \\ h[\overline{I(v)_n}] + \xi(G_{max} - G(v)) + GD(v) & \text{for external nodes} \end{cases} \quad (5)$$

where the symbols have the same meaning as in equation 4.

The segmentation process consists of several stages. First, a mesh with an homogeneous distribu-

tion of nodes is created and located over the whole image. Then, the mesh energy is minimised iteratively using a greedy algorithm. The energy functions reach a minimum when the mesh is located around the objects. After that, the number of nodes in each axis is recomputed to adapt the mesh size to the object size; for example, if the object is longer than wider, the number of nodes in the x-axis will be increased whereas the number of nodes in the y-axis will be decreased. The mesh is also centred over the detected objects and its energy is minimised again. Finally, topological changes are performed to increase the flexibility of the model and, after a local energy minimisation step (Barreira et al., 2006), to adjust the mesh to concave surfaces, holes, or separate objects.

The topological changes involve the breaking of links between external nodes wrongly located, this is, external nodes far away from the objects. These nodes are identified and sorted by their distance to the objects in order to break the links between the worst located nodes (Barreira and Penedo, 2005). However, some link breakings are not allowed because of the fact that the mesh should keep the polyhedral structure since isolated nodes or planes does not provide volumetric information.

3 TETRAHEDRAL MESHES

The TAV model has been developed using a cube as the base polyhedron of the mesh. Even though the segmentation results using this configuration were good (Barreira and Penedo, 2004), the topology based on cubes has limitations in the adjustment to surfaces. Specifically, the four-sided faces of the cubes have difficulty in the adjustment to pronounced curvatures. Although this problem can be partly solved by increasing the density of nodes, a new mesh topology that could improve the segmentation results is necessary. Figure 2 shows the reconstruction of an object with several small holes that the cubic topology is not able to detect with a small mesh size and detects roughly with a larger mesh size.

The triangular meshes have the advantage of being able to model very complex geometries so that they can improve the results of a quadrilateral mesh. Therefore, most of the surface reconstruction techniques use triangular meshes to represent surfaces. Since the TAV model works in 3D with polyhedra, the new mesh topology will consist of triangle-based polyhedra, this is, tetrahedra.

Given that there are five tetrahedra in a cube (see figure 3), the tetrahedral mesh is built from a cubic mesh in such a way that each cube is the specular im-

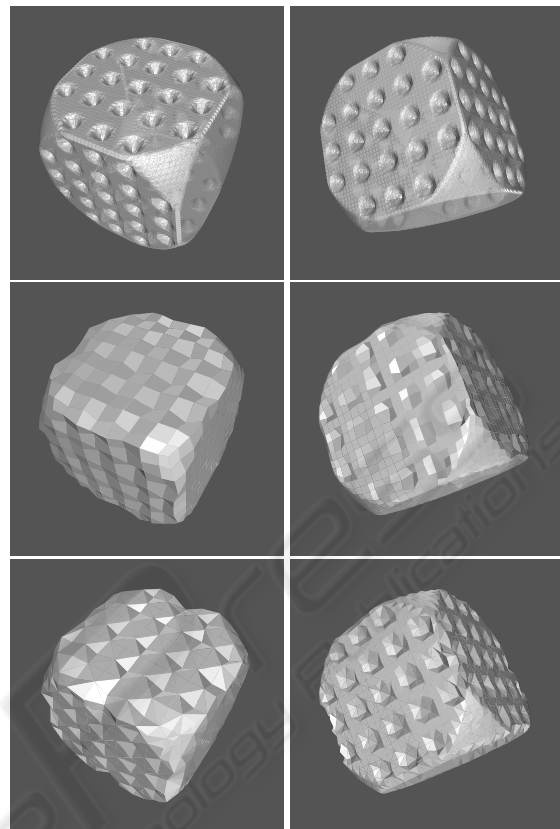


Figure 2: Adjustments of meshes based on cubes and tetrahedra. First row: original object. Second row: results using a cubic mesh. Third row: results with tetrahedral meshes. The meshes have $10 \times 10 \times 10$ nodes in the first column and $20 \times 20 \times 20$ in the second one. The tetrahedral mesh is able to detect the small rounded holes in the surface of the object even with the $10 \times 10 \times 10$ mesh. On the contrary, although the results are improved when the mesh size is increased, the cubic mesh only detects roughly the holes with the $20 \times 20 \times 20$ mesh.

age of its neighbours. Figure 4 shows an example of a tetrahedral mesh with $3 \times 3 \times 3$ nodes.

The mesh topology change does not affect the segmentation process whereas the accuracy of the results is improved as figure 2 shows. Nevertheless, the new neighbourhood of the nodes will affect the calculus of the external energy function (see eq. 3) in the minimisation stage. Since the number of neighbours grows in the tetrahedral meshes and the calculus of the external energy depends on the neighbourhood, the tetrahedral meshes will be slower than the cubic meshes.

In order to speed up the adjustment process and given that the cubic meshes often produce good results, a mixed approach has been developed in this paper. In this approach, the segmentation process starts with a cubic mesh. Its energy is minimised and, after that, its size is recomputed. When the minimisation

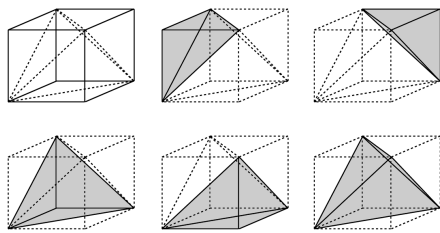


Figure 3: Decomposition of a cube in five tetrahedra. The tetrahedral mesh is built from this decomposition and its specular image.

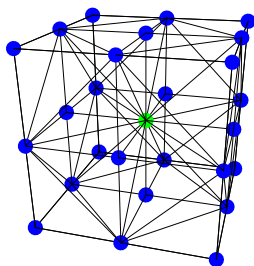


Figure 4: A tetrahedral mesh with $3 \times 3 \times 3$ nodes. The dark nodes are the external nodes whereas the light central one is the internal one.

process finishes for the second time, the cubic mesh is able to detect the objects but maybe an improvement in the adjustment is needed. At this point, a tetrahedral mesh is built from the adjusted cubic mesh and its energy is minimised again. This way, the cubic mesh obtains a coarse but fast segmentation whereas the tetrahedral mesh achieves a fine adjustment. Figure 5 shows how the mixed approach is also able to detect the small holes in the object in figure 2 as accurately as the tetrahedral approach.

Regarding the topological changes, only breakings that preserve the tetrahedral structure are allowed. To this end, the mesh integrity is checked

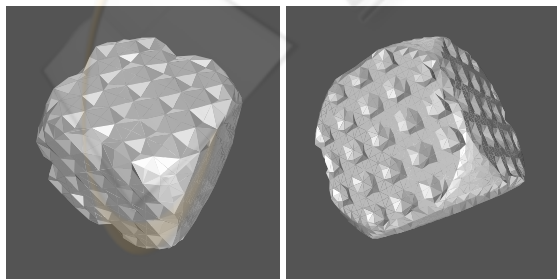


Figure 5: Adjustments of the mixed approach. Left image was segmented with a $10 \times 10 \times 10$ mixed mesh and the right one, with a $20 \times 20 \times 20$ mesh. The results of both tetrahedral and mixed approaches are equivalent.

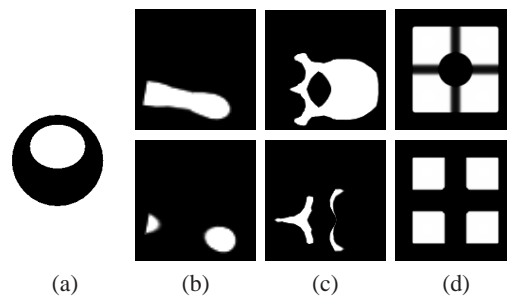


Figure 6: Some slices of the 3D images used in the examples. Slices (a), (b), (c), and (d) correspond to the images in figures 7, 8, 9, and 10, respectively.

Table 1: Parameters used in the examples.

Figures	α	β	γ	ρ	ω	ξ
7	1.5	10^{-5}	10^{-5}	3.0	3.0	5.0
8	3.5	10^{-5}	10^{-5}	4.0	3.0	6.0
9	2.0	10^{-4}	10^{-4}	4.0	4.0	6.0
10	3.0	10^{-5}	10^{-5}	3.0	3.0	5.0

before each breaking. This way, a link between two nodes is broken only if all their neighboring nodes belong to, at least, another tetrahedron after the link breaking.

4 RESULTS

This section shows the results of applying the tetrahedral meshes to several synthetic images. A 3D image is built as a set of 2D stacked images. Figure 6 shows some slices of the images used in the segmentation examples. The input image was used in the calculus of the external energy for both internal and external nodes. The gradient images were computed using a 3D Canny detector. The model parameters, empirically chosen, are summarised in table 1. Since the mixed strategy is faster than the tetrahedral approach and produces similar results, all the tetrahedral results in this section were obtained using the mixed strategy.

The efficiency and the adjustment of the topologies developed were analysed. With this aim, several segmentation processes with different mesh sizes were performed and the computation times of the cubic, tetrahedral, and mixed approaches were compared. The processes were run in an Intel Core 2 Duo at 2.40 GHz. The graphs in figures 7, 8, and 9 show the computation times of the adjustment processes, prior to the stage of topological changes, for three example images. The graphs show that not only the computation times of the mixed segmentations

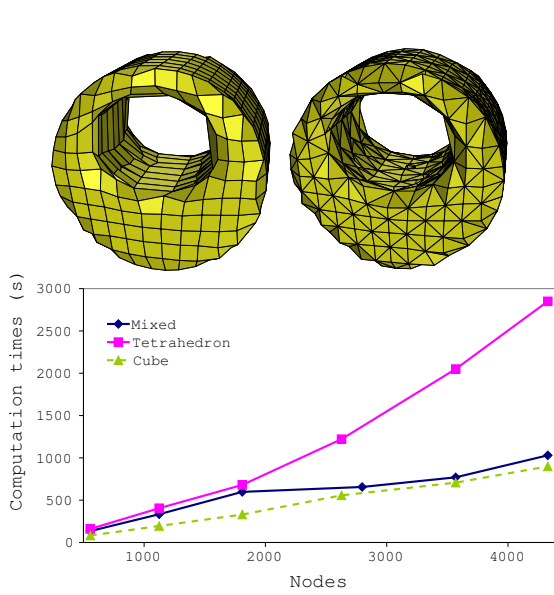


Figure 7: Segmentation results in a synthetic image. Top: results of the cubic (left) and the mixed (right) approaches. In both cases, the initial meshes had $10 \times 10 \times 10$ nodes. Bottom: evolution of the computation times of the mesh topologies with respect to the average mesh size of the initialisation and readjustment stages. The tetrahedral mesh produces a more accurate adjustment to the hole surfaces.

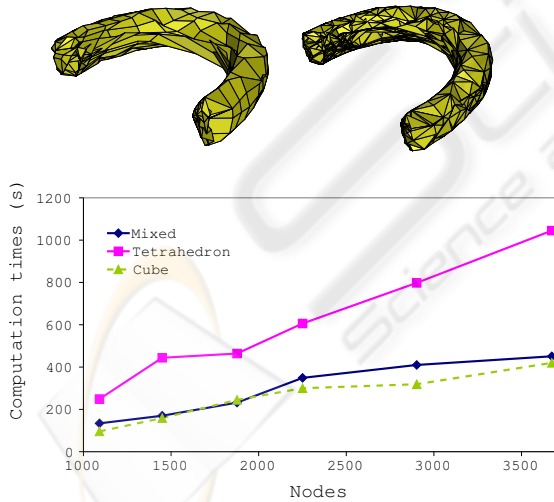


Figure 8: Segmentation of a synthetic object. Top: results with an initial $9 \times 9 \times 9$ cubic mesh (left) and an initial $12 \times 12 \times 12$ mixed mesh (right). Bottom: evolution of the computation times of the mesh topologies with respect to the average mesh size of the initialisation and readjustment stages. The adjustment of the tetrahedral mesh is more accurate in the concave area.

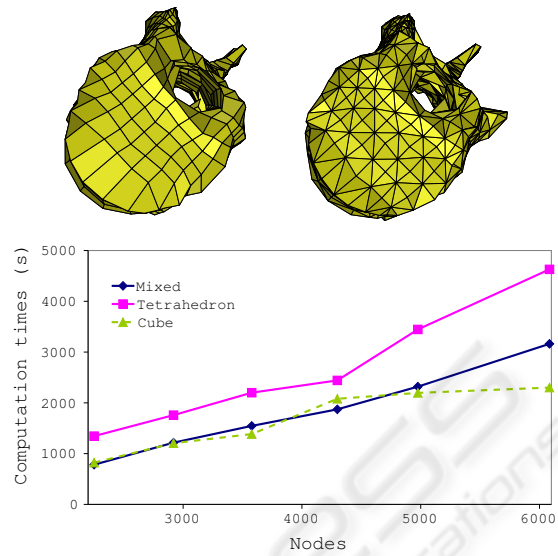


Figure 9: Segmentation of a vertebra. Top: results of the cubic (left) and mixed (right) approaches. The initial meshes had $13 \times 13 \times 13$ nodes. Bottom: evolution of the computation times of the mesh topologies with respect to the average mesh size of the initialisation and readjustment stages. The tetrahedral mesh produces better results since it detects both lateral prominent areas of the vertebra.

are lower and similar to the cubic ones, but also the time increase as the mesh size grows is greater in the case of the tetrahedral meshes. Also, the tetrahedral meshes improve the adjustment to surfaces.

Figure 10 shows a special case where the object covers almost the whole image. In these cases, the mixed strategy produces higher computation times than the cubic approach. The mixed approach only uses the fast cubic approach to detect the objects. For this reason, when the objects cover the whole image, the cubic step is very short and the adjustment is achieved mainly by means of the tetrahedral mesh. This way, the computation times for both mixed and tetrahedral approaches are similar. Nevertheless, the improvement in the surface adjustment justifies the use of a tetrahedral mesh.

5 CONCLUSIONS

This paper proposes a new topology for the Topological Active Volumes model. The former TAV topology based on cubes has limitations to achieve a fine adjustment to curved surfaces. For this reason, a new topology based on tetrahedra was developed. The new topology behaves like the cubic one, this is, the tetrahedral topology is able to detect several objects in the scene and to adjust to object concavities and holes.

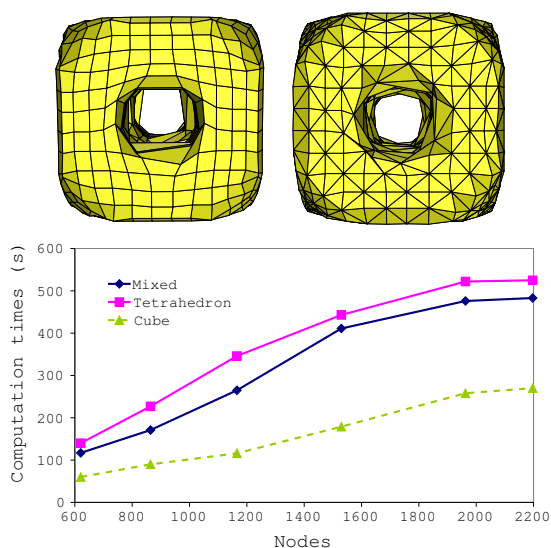


Figure 10: Segmentation of a cube with holes. Top: segmentation results with a cubic mesh (left) and a mixed (right) mesh of $11 \times 11 \times 11$ nodes. Bottom: evolution of the computation times of the mesh topologies with respect to the average mesh size of the initialisation and readjustment stages. The mixed and tetrahedral approaches have similar computation times because the object covers the whole image.

However, the new relationships between nodes in the tetrahedral meshes imply a higher complexity in the segmentation process as well as an increase in the computation time. In order to overcome these drawbacks, a new strategy was proposed. A mixed topology that combines a cubic mesh for a fast and rough segmentation and a tetrahedral mesh for a fine adjustment. This strategy not only reduces the computation times, but also improves the results of the segmentation process.

Future work includes the development of techniques to change the structure of the tetrahedral mesh by means of inserting or removing nodes in order to achieve a fine adjustment to complex areas.

ACKNOWLEDGEMENTS

This paper has been partly funded by the Xunta de Galicia through the grant contracts PGIDIT05SIN001E and PGIDIT06TIC10502PR.

REFERENCES

- Archip, N., Rohling, R., Dessenne, V., Erard, P.-J., and Nolte, L.-P. (2006). Anatomical structure modeling from medical images. *Computer Methods and Programs in Biomedicine*, 82(3):203–215.
- Barreira, N. and Penedo, M. G. (2004). Topological Active Volumes for Segmentation and Shape Reconstruction of Medical Images. *Image Analysis and Recognition: Lecture Notes in Computer Science*, 3212:43–50.
- Barreira, N. and Penedo, M. G. (2005). Topological Active Volumes. *EURASIP Journal on Applied Signal Processing*, 13(1):1937–1947.
- Barreira, N., Penedo, M. G., and Penas, M. (2006). Local energy minimisations: An optimisation for the topological active volumes model. In *First International Conference on Computer Vision Theory and Applications*, volume 1, pages 468–473.
- Kass, M., Witkin, A., and Terzopoulos, D. (1988). Active contour models. *International Journal of Computer Vision*, 1(2):321–323.
- Pons, J.-P. and Boissonnat, J.-D. (2007). Delaunay deformable models: Topology-adaptive meshes based on the restricted delaunay triangulation. In *IEEE Conference on Computer Vision and Pattern Recognition*, Minneapolis, USA.
- Sermesant, M., Forest, C., Pennec, X., Delingette, H., and Ayache, N. (2003). Deformable biomechanical models: Application to 4D cardiac image analysis. *Medical Image Analysis*, 7(4):475–488. PMID: 14561552.
- Sitek, A., Huesman, R., and Gullberg, G. (2006). Tomographic reconstruction using an adaptive tetrahedral mesh defined by a point cloud. *IEEE Transactions on Medical Imaging*, 25(9):1172 – 1179.
- Terzopoulos, D., Witkin, A., and Kass, M. (1988). Constraints on deformable models: Recovering 3D shape and nonrigid motion. *Artificial Intelligence*, 36(1):91–123.
- Tsumiyama, K. and Yamamoto, K. (1989). Active net: Active net model for region extraction. *IPSJ SIG notes*, 89(96):1–8.